Macro scale (1:50,000) landslide susceptibility mapping in parts of Kullu and Mandi districts, Himachal Pradesh

Lakshmanan. K.,

Senior Geologist, Engineering Geology-II and Landslide Division, Geological Survey of India, Sector 33B, Chandigarh-160020

Mandal, Jina

Senior Geologist, Engineering Geology-II and Landslide Division, Geological Survey of India, Sector 33B, Chandigarh-160020

Jayabalan. K.,

Deputy Director General, GHRM Cell, Geological Survey of India, 27 J.L. Nehru Road, Kolkatta-760016, West Bengal, India

Kumar, Manoj

Director, Engineering Geology-II and Landslide Division, Geological Survey of India, Sector 33B, Chandigarh-160020

Abstract

Rapid urbanization in developing high relief terrains has many irreversible geo-environmental impacts resulted in the form of landslides. They not only caused damage to properties and life, but also affect the socio-economic growth of the area by disrupting the utility services and economic activities. Himachal Pradesh is well known for its eye catching scenic beauty. Kullu and Manali are the two eminent hot spots that attract thousands of tourists from different parts of world throughout the year beside Beas River. Chandigarh-Manali National Highway NH-21 is a strategically important communication route that connects passes through thickly habituated townships such as Kullu, Bhuntar, Bajaura, Larji and Pandoh. This highway witnesses quite many landslides that include recent Dwada landslide (2015 & 17). Considering the importance of the route and area, landslide susceptibility study has been carried out by calculation of Yule's Co-efficient and Landslide Occurrence Favorability Score (LOFS), determination of weightage for factor class by Weighted Multiclass-index Overlay Method to categorize landslide susceptible slopes. The rating maps were integrated in GIS to obtain susceptibility score map, which finally classified into 'high', 'moderate' and 'low' based on cumulative distribution of landslides, using 'success rate curve'. The susceptibility map with landslide incidence classifies the area into qualitative landslide susceptibility map indicating areas of "High", "Moderate" and "Low" susceptibility classes.

Keywords: Landslide, Susceptibility, Weighted index, Kullu.

1. Introduction:

Landslide disasters in Himalayan terrain have made tremendous adverse socio-economic impact in the recent past. As a result of increasing urbanization, hill slopes are increasingly becoming unstable. Landslides are one of the significant destructive geological processes which frequently cause enormous damage to lives and property (Ghosh et al. 2014). Hence, need for landslide susceptibility mapping has always been felt with regards to identification of potential landslide areas (Sarkar and Kanungo, 2004). Landslide susceptibility mapping is useful for delineating the potential landslide zones (Sarkar et al. 2006). GIS based landslide hazard zonation studies are effective techniques to negotiate and mitigate landslides (Anbalagan, 1996) (Chandel et al). There

are plenty of methods of predictive mapping of landslide susceptibility. Landslides have complex interactions with several geo-environmental spatial factors (Guzzetti et al., 1999; van Westen et al., 2006). The fundamental assumption is spatial factors that caused present and past landslides are likely to cause similar landslides in the future (Varnes, 1978; Guzzetti et al., 1999). Weighted Multi-class Index Overlay Method (Guzzetti et al., 1999; van Westen et al., 2006, Ghosh et al., 2011) has been used in the present study for landslide susceptibility mapping.

1.1 Location and Accessibility:

The study area encompasses parts of Kullu and Mandi districts of Himachal Pradesh and falls under T.S. nos. 53E/01 and 53E/02 located on the banks of the Beas River. The total area is bounded by latitudes 31^0 30' 00" to 32^0 00' 00" N and longitude 77^0 00' 00" to 77^0 15' 00" E covering a total area of 1313.4 km^2 in parts of Kullu and Mandi districts, Himachal Pradesh. The study area is well connected by road and air routes. Kullu, Bhuntar, Mohal, Bajaura, Panarsa and Aut are some of the main towns in toposheet no. 53E/01 of district Kullu and Pandoh, Chail Chauk, Chachyot and Jhanjheli are some of the main towns and localities in toposheet no. 53E/02 under Mandi district.

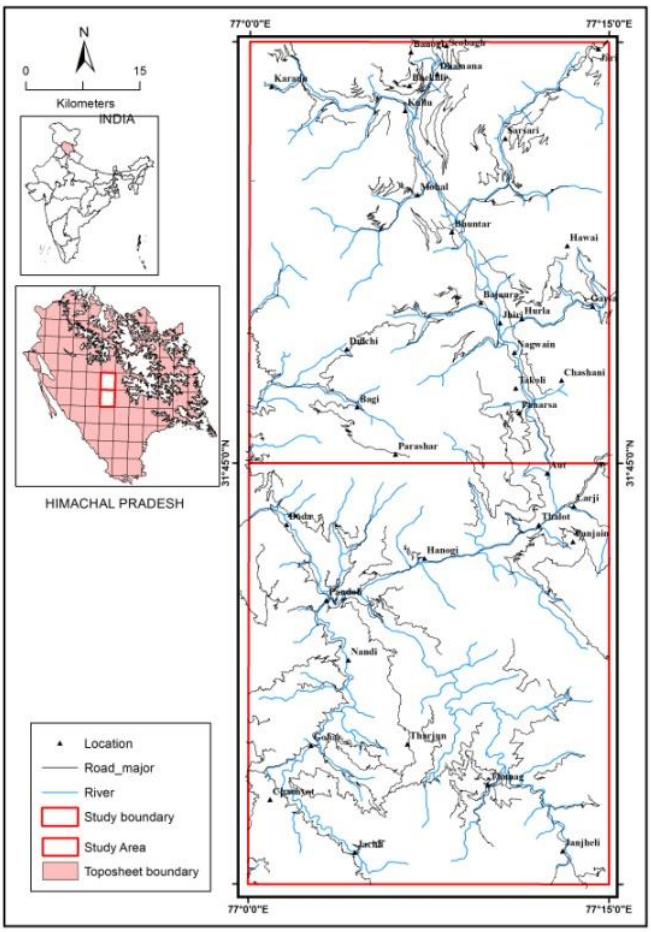

Figure 1 Location map of the study area

2. Geology of the Himalayas:

The study area forms a transitional zone between the Lesser Himalayas and is characterized by high NW-SE trending ridges and deep river valleys. The altitudes vary from 950m to 6000m. Geologically, the study area is represented by rock sequence ranging from Paleo-Proterozoic to Neo-Proterozoic (Bhargava and Bassi, 1994). A broad central zone of crystalline rocks consisting of granite, gneisses, schist and other metamorphic rocks forms the axis of the Himalayas (Kayastha, 1964). Five major litho-tectonic units express the geology of the area and these are referred to as (1) Vaikrita Group (2) Jutog Group (3) Kullu Group (4) Larji Group and (5) Rampur Group. The area is dissected by several major thrusts namely Jutogh Thrust, Kullu Thrust and Vaikrita Thrust along with several local faults/lineaments. These thrusts are still active and play a major role in the neo-tectonics of the area (Choubey et al., 2007) defines boundary between the rocks of Rampur, Larji and Kullu groups. Structurally, the main Kullu valley is a gently folded antiform having River Beas following its axial plane along a fault running NNW-SSE from the upper catchment to near Aut where it is intersected by a cross fault almost at right angles (Sah & Mazari, 2007) (Das et al. 1979). This fault is a dextral tear fault with a dislocation of nearly 1.5 km (Shankar & Dua, 1978). The rivers Beas, Parvati, Hurla Nala, Sainj Khad, Tirthan Khad etc. follow such fault traces. The area west of river Beas from Bhuntar and south of Parvati River to Rampur along the course of Satluj River forms 'window in a window' structure also known as Kullu-Larji-Rampur Window.

3. Methodology:

In this study the landslide susceptibility maps were prepared from nine geofactor /thematic maps by Weighted Multi-class Index Overlay Method (Guzzetti et al., 1999; van Westen et al., 2006, Ghosh et al., 2011). The geofactor maps are slope morphometery map, slope aspect map, slope curvature map drainage map (Aster DEM derivatives prepared in ArcGIS). These were used as landslide inventory data for analysis. Apart from this Geomorphology map, Land use and Land cover map (LULC), Slope Forming Material map (SFM), structural map (Fault / thrust) and landslide incidence/inventory map were prepared using both remote sensing data and fieldwork, taking into account all the past known events. The flow diagram showing the process for Landslide Susceptibility Mapping is displayed below (Figure 3).

For validation, the resulting landslide susceptibility map was combined with the landslide inventory map. The success rate curve was prepared by plotting the cumulative percentage of all known landslide area (along y-axis) versus the cumulative percentage of the area of the susceptibility map, ordered from high to low susceptibility score values following method proposed by Chung and Fabbri (2003). If the success rate rate curve is steep at lower cumulative map area percentage of highest score values, then the landslide susceptibility map has strong ability to predict areas that are most susceptible to landslides.

The Weighted Multiclass Index Overlay method is the improved bivariate statistical method for defining landslide susceptibility (Ghosh, 2011). Given that a categorical spatial factor map (f) is multi-class and a landslide occurrence map (s) is binary, the measure of the spatial association between classes of f and s is calculated by the Yule's coefficient (Y_C) (Yule, 1912; Fleiss, 1991; Bonham-Carter, 1994):

$$Y_C = \frac{\sqrt{M_{fs}/M_{\bar{f}s}} - \sqrt{M_{f\bar{s}}/M_{\bar{f}\bar{s}}}}{\sqrt{M_{fs}/M_{\bar{f}s}} + \sqrt{M_{f\bar{s}}/M_{\bar{f}\bar{s}}}}, \qquad \text{Eq. (1)}$$

where Mfs is area of 'positive match' where a factor class and landslides are both present, $M_{\bar{f}s}$ is area of 'mismatch' where a factor class is absent but landslides are present, $M_{f\bar{s}}$ is area of 'mismatch' where a factor class is present but landslides are absent, and $M_{\bar{f}\bar{s}}$ is area of 'negative match' where a factor class and landslide are both absent. The value of Y_C ranges between –1 and +1. A negative Y_C means negative spatial association, whereas a positive Y_C means positive spatial association.

Based on Y_C, for each factor class a Favorability Score or rating (F_{Ct}) is derived:

$$F_{Ct} = \begin{cases} 0 & for \quad Y_C \le 0 \\ Y_C / Y_{C_{\max}} & for \quad Y_C > 0 \end{cases} \qquad \text{Eq. (2)}$$

where, $Y_{C_{\max}}$ is the highest Y_C of all classes in a spatial factor and F_{Ct} represents the relative degree of influence of every factor class on the susceptibility to landslide occurrence in the range of 0 to 1.

Individual spatial factors can have different degrees of spatial associations with landslides. However, as land sliding is related an inter-play of multiple factors, predictive modeling of SL requires analysis of inter-predictor weights. To determine the relative importance of every predictor, a predictor rating (PR) for every spatial factor based on their degree of spatial association with landslides can be determined:

$$PR = |SA_{\max} - SA_{\min}| / |SA_{\max} - SA_{\min}|_{\min} \qquad \text{Eq. (3)}$$

where SA is the degree of spatial association (Y_C for categorical variables) of classes of a spatial factor with a set of landslides. For each factor the absolute difference between the maximum and minimum SA values is calculated, which is then divided by the lowest absolute difference of all the factors to obtain the inter-predictor weights. To integrate the selected predictors for landslides, the weighted multi-class index overlay method (Bonham-Carter, 1994) can be applied. In each of the i-th (i = 1,2,…,n number of) predictor maps, each of the j-th (j = 1,2,…,m number of) predictor classes is assigned a favorability score (F_{ji}) obtained through spatial association analysis. Every i-th predictor map is assigned an integer predictor weight, Wi, obtained through calculation shown above. Weighted predictor maps are then combined using the following equation, which

calculates an average weighted score of landslide susceptibility ($\overline{S}$) for every location/ pixel (Bonham-Carter, 1994):

$$\overline{S} = \Sigma_i^n (F_{ji} \times W_i) \Big/ \Sigma_i^n W_i \qquad \text{Eq. (4)}$$

The output map of $\overline{S}$ is a predictive model of landslide susceptibility to occurrence of landslides under examination in the area. Success rate curve, as proposed by Chung and Fabbri (2003) is used subdivide the landslide scores into three classes of different landslide susceptibility (i.e., high, moderate and low). The cut-off boundaries are taken based on cumulative distribution of landslide percentage such that 80% landslides are contained within high susceptibility and 90% in moderate susceptibility.

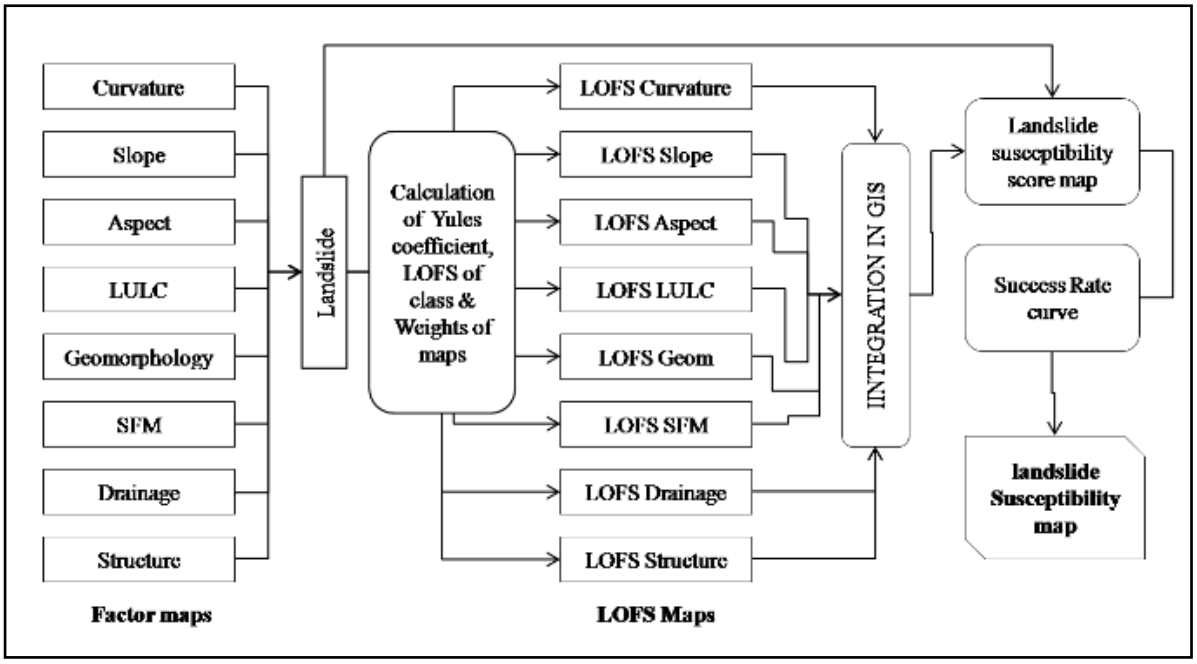

Figure 3 Flow diagram showing the process for Landslide Susceptibility Mapping.

3.1 Data Source:

The following sources were used for the preparation of Geofactor maps:

Table 1
List of Data Source

Remote Sensing Data	**Ground Data**
ASTER DEM	SOI topo sheets
Multi temporal Google Earth images / Arc GIS Geoeye image	GSI Geological maps on 1:50000 scale
LISS-III	Available landslide inventory reports

The landslide susceptibility map was prepared in raster format, using pixel of 50m x 50m grid as a mapping unit and by calculating the Landslide Occurrence Favorability Score (LOFS) for all factor classes in ArcGIS. A susceptibility score map is calculated after adding LOFS values of all eight factor maps and normalizing it by its weight. Success rate curve (Chung and Fabbri, 1999) is used to subdivide the susceptibility scores into three classes of different landslide susceptibility (i.e., high, moderate and low). The cut-off boundaries are taken based on cumulative distribution of landslide percentage such that 80% landslides are contained within high susceptibility and 90% in moderate zone (Fig 3.2).

4. Analysis of Results and Discussion:

Landslide susceptibility is a quantitative of quality and guesstimate of the spatial prevalence distribution of landslides, which exist or potentially may occur in an area. Although it is expected that landslides may occur more frequently in the most susceptible areas, however, in the susceptibility analysis, no time frame and magnitude of event are explicitly taken into account. A susceptibility map therefore gives only the qualitative or quantitative estimation that the mapping unit (e.g., a pixel, slope unit or facet) will be affected by a future landslide source.

4.1. Susceptibility Analysis:

The factor class ratings and inter predictor weights of factor maps using landslides as dependent variable are as follows:

i. The landslide inventory (Fig. 3.2), LULC, Geomorphology and SFM digitized as a polygon shape file, were converted into rater maps of 50m × 50m pixel size. Drainage and structure maps, digitized as a polyline shape file, were converted into raster maps of 50m × 50m pixel size.
ii. The ASTER DEM derivatives such as slope, aspect and curvature were reclassified into categorical variables. Slope map was reclassified into 10 classes as per 10 percentile distribution; aspect map into 12 classes with 30° increment and curvature into 5 classes.
iii. The number of landslide pixels in each factor maps was calculated using the 'combine' function in Arc GIS. The calculation of the ratings for each factor class and weights of each factor map was performed in Excels. The tables obtained after combining the landslide and factor maps provided the value for the number of landslide pixels (npixd) in each class and total pixel of that particular factor class (npixc).
iv. For each factor class, first the Yule's coefficient (Y_C) was calculated in Excel using Eq. (1). From Y_C, the Landslide Occurrence Favorability Score (LOFS) rating is calculated by dividing the Y_C value by its maximum to restrict the LOFS between 0 and 1 give the obtained LOFS ratings of all factor classes of the respective nine thematic maps. The excel table is joined with the factor maps using the 'table join and relate' function in Arc GIS.

v. The predictor rating (PR) for every spatial factor based on their degree of spatial association with landslides is calculated using Eq. (3). The obtained value is converted into integer by dividing each by the maximum value. Table 4.8 gives the weight values of each factor map.
vi. Using 'map algebra' function in Arc GIS the obtained rating maps were combined together following the Eq. (4) to obtained landslide score maps.
vii. Success rate curve function is used to subdivide the landslide scores into three classes of different landslide susceptibility (i.e., high, moderate and low). The cut-off boundaries are taken based on cumulative distribution of landslide percentage such that 80% landslides are contained within high susceptibility and 90% in moderate susceptibility and rests in low class (Fig 4.1).

4.2 Geofactor maps and their feature class distribution in the área:

The study area exhibits predominance of slope morphometery angle classes 25° to 35° constituting 50% of the total area (Fig 4.2.a), whereas maximum nos. of landslide (193 nos) are associated with slope class 35° followed by 30° and 40°. Further analysis indicated that maximum favorable slope class is 35° - 40° as indicated by LOFS values of 1 (Fig 4.2.b). Aspects classes have nearly equal distribution of various classes in the area. The SSE slope aspect class with minimum area distribution but is associated with maximum nos. of landslides (Fig 4.3.a & b). The slope class also revealed to be most favorable for landslide as indicated by the LOFS value of (1). The curvature maps were reclassified into five classes and the analysis reveals that the study area exhibits predominantly concave (45%) followed by convex (43%) and flatter terrain 12% (Fig 4.4.a). LULC map was grouped into 12 classes as given in and the most abundant class is the agricultural land that covers about 33% area, followed by thick vegetation and moderate vegetation covering 32% and 21% area respectively (Fig. 4.5.a). Majority of the landslides (49%) occurred within extensive slope cut (Fig. 4.5.b). This is followed by agricultural land and barren rocky slope. The graphical plot of LOFS against Yules coefficient reveals that most favorable geofactor classes for the landslides to occur are extensive cut slopes and toe erosion (Fig. 4.5.b)

Moderately dissected hill (23.5%) class is predominance of Geomorphology geofactor in the study followed by low dissected hill and transformational mid slopes of 23% and 13% respectively (Fig. 4.6.a). The correlation study between LOFS and Yule's coefficient reveals that the denudational hill slope favors for landslide occurrence with score 1(Fig. 4.6.b). The spatial distribution of soil/overburden and its thickness is controlled by erosional processes and slope morphometery (Dietrich et al., 1986; De Rose et al., 1991). The SFM categories constituting 30% of the total study area followed by older well compacted debris 13% (Fig. 4.7.a). The correlative study of LOFS with Yule's coefficient reveals that the highest rating 1 for the geofactor highly joint and fractured rock mass (Fig. 4.7.b). The drainage buffer study indicates that drainages with 1000m and 2000m buffer distance are with higher number of pixels in the study area (Fig 4.8.a). However closer drainage buffer distance with100m has the strong control on landslides in the area (Fig 4.8.b).

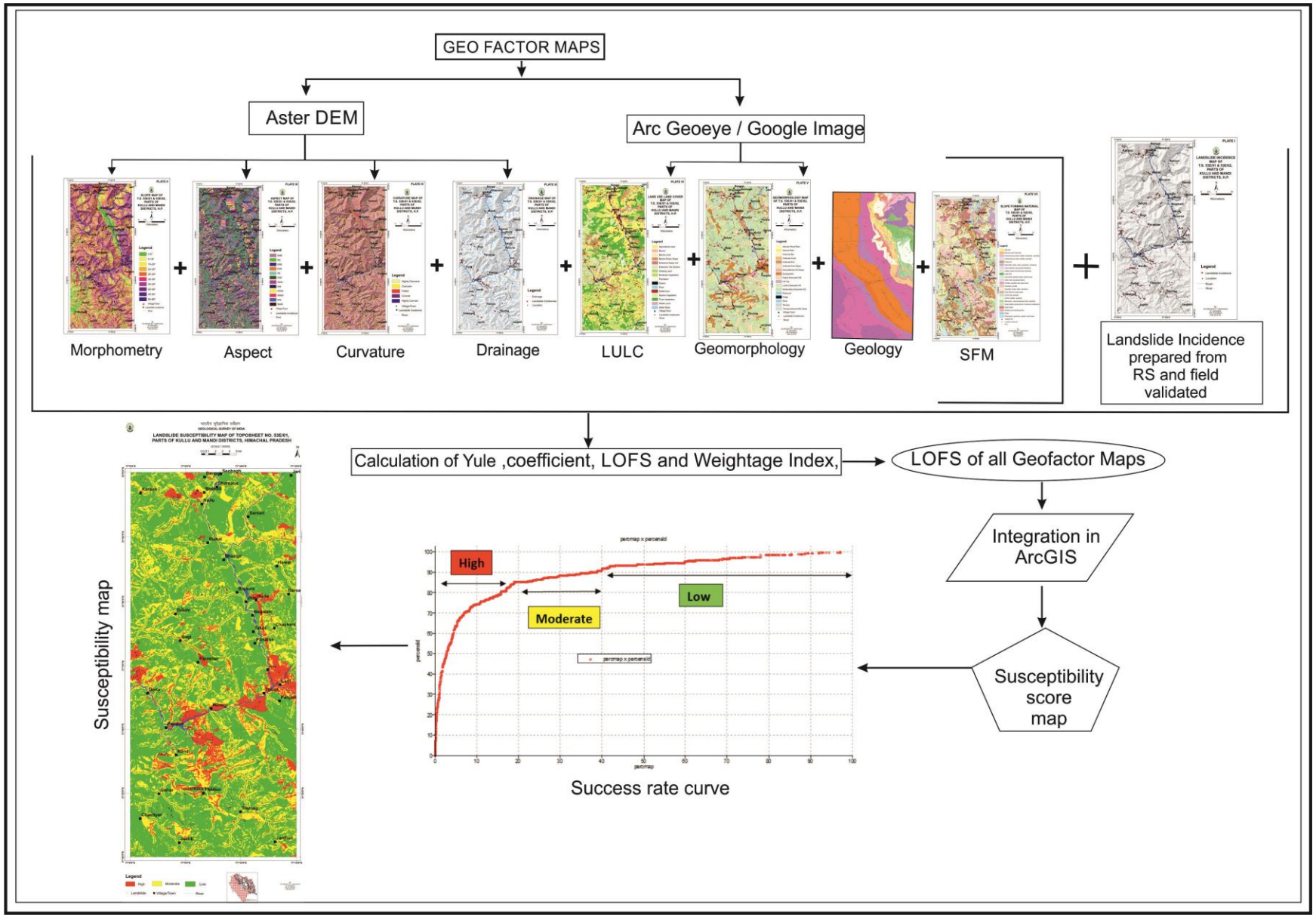

Figure 4.1 Steps involved in preparation of Landslide Susceptibility map

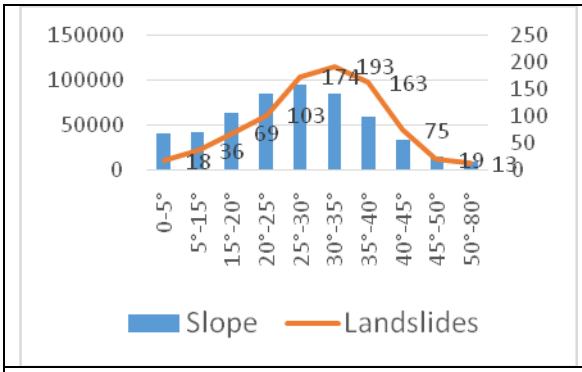

Fig 4.2.a: Predominance of slope angle class in the area

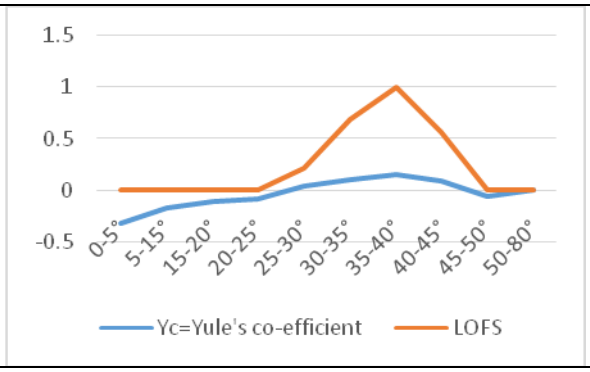

Fig 4.2.b: Maximum favorable slope class is 35° - 40° as indicated by LOFS values

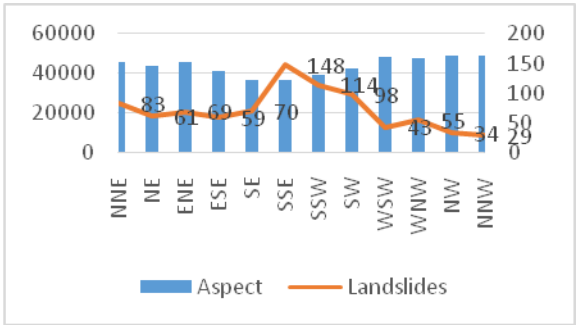

Fig 4.3.a SSE slope aspect class with minimum area distribution but is associated with maximum nos.of landslides

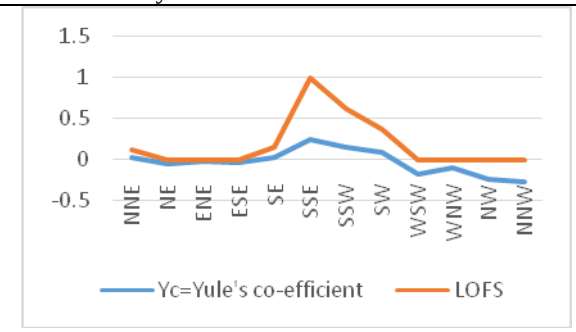

Fig 4.3.b SSE slope aspect class most favorable for landslide as indicated by the LOFS value of (1)

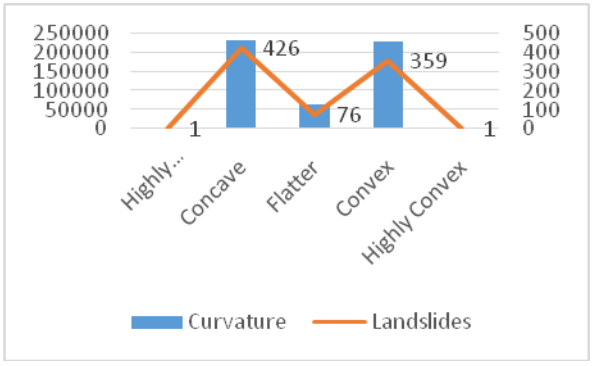

Fig 4.4.a Distribution of curvature classes

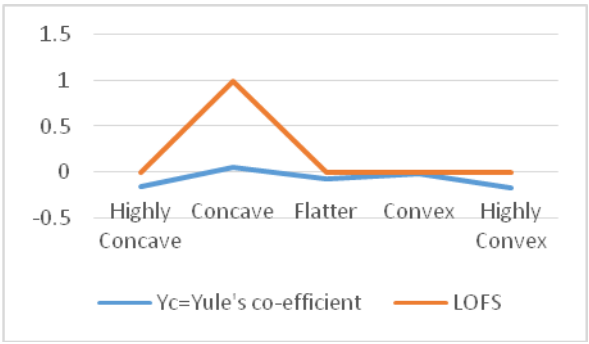

Fig 4.4.b Concave class favorable for landslides occurence

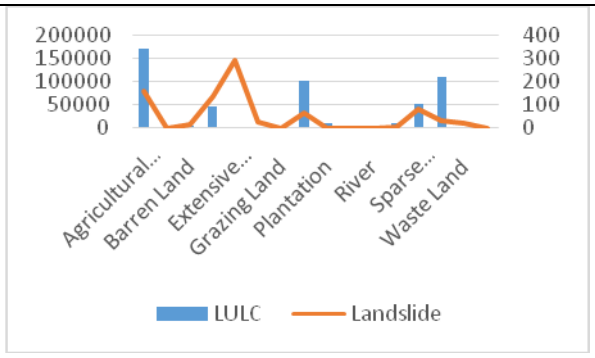

Fig 4.5.a. Distribution of LULC classes in the area

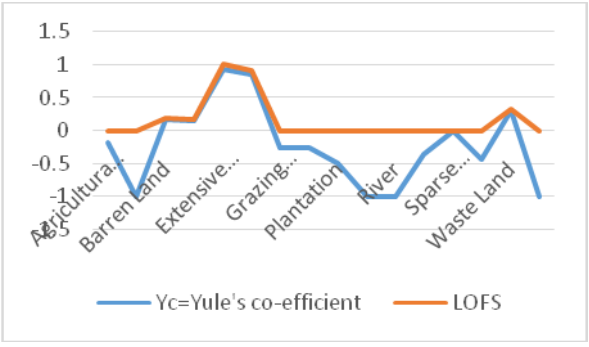

Fig 4.5.b. High LOFS value for extensive slope cut

	class
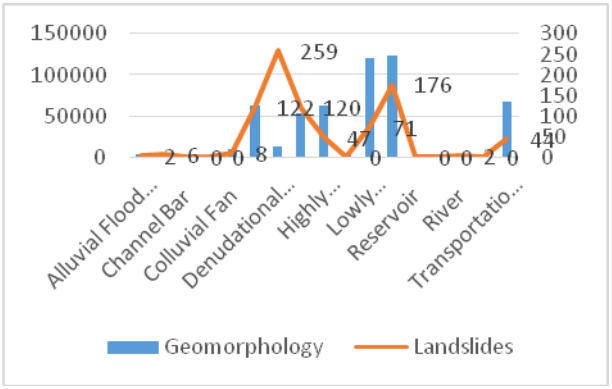	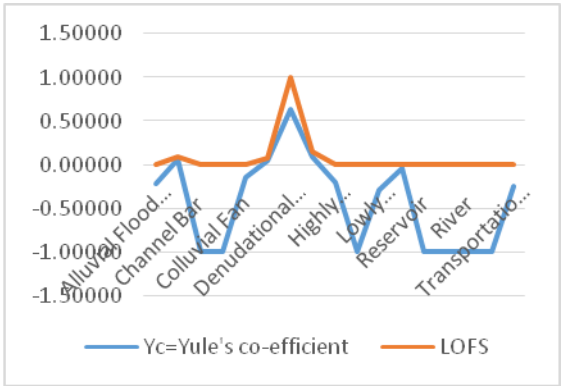
Fig 4.6.a. Distribution of Geomorphology classes in the area	Fig 4.6.b. High LOFS value for Denudational hill class
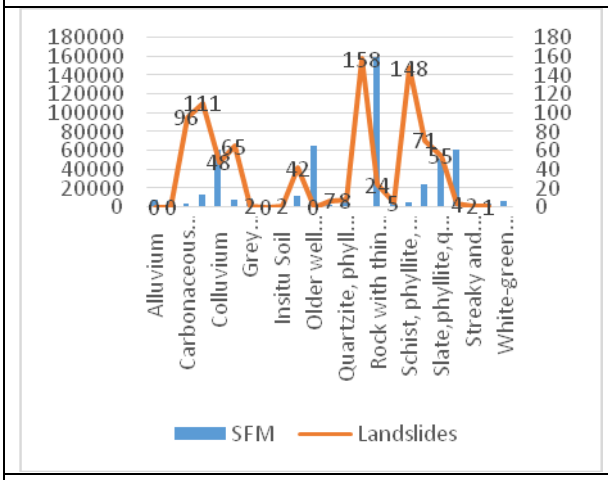	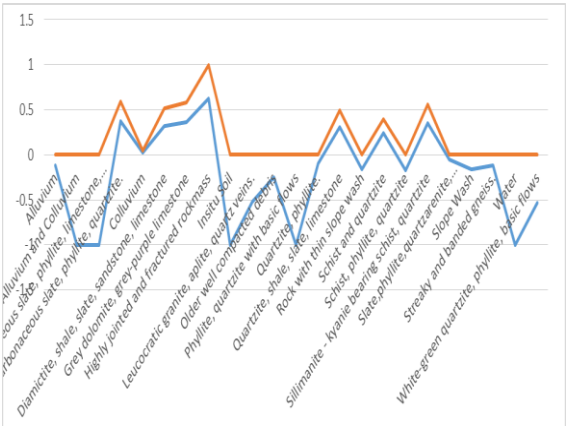
Fig 4.7.a Distribution of Geomorphology classes in the area	Fig 4.7.b. High LOFS value for Highly jointed and fractured rock mass class
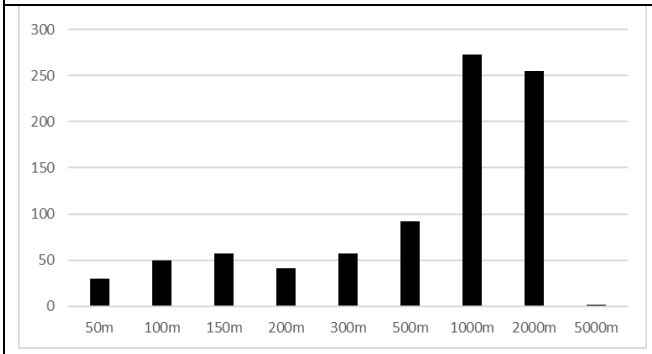	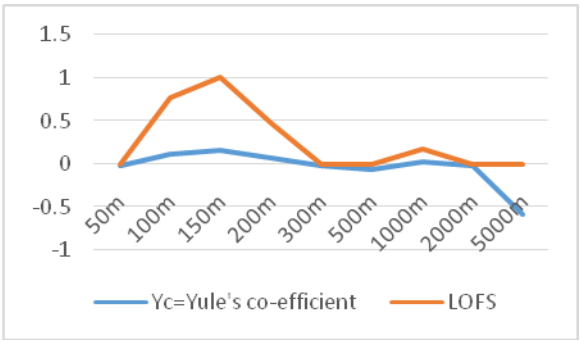
Fig 4.8.a Distribution of Geomorphology classes in the area	Fig 4.8.b High LOFS value for 150m buffer distance

4.3. Landslide Susceptibility Map:

Using all the nine geo-factor maps and Eq. (4), a landslide susceptibility score map was generated. The obtained score map was combined with the landslide map and a Success Rate Curve was generated in ILWIS 3.2, following the method proposed by Chung and Fabbri (2003). The obtained success rate curve is shown in Fig. 5. The Success Rate Curve revealed that about 85% cumulative distribution of all landslide source areas is contained within 20% of the study area having High susceptibility scores. The next 90% of cumulative landslides are contained within 40% of the study area, defining Moderate zone. The susceptibility score values at the cut off boundary of cumulative 85% and 90% landslides are taken for defining the boundary limit of High and Moderate susceptibility class

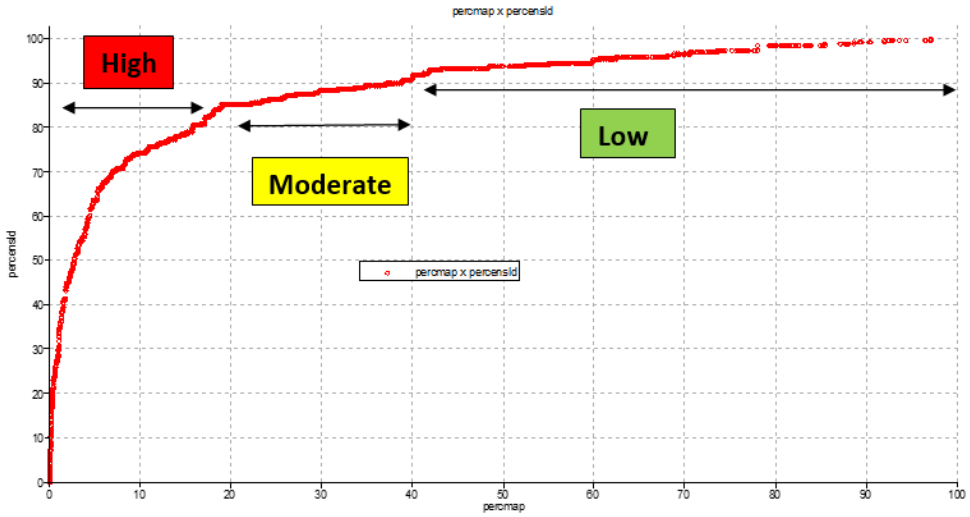

Figure 5 Success Rate Curve depicting limits for high, moderate and low

4.4. Susceptibility zones of the study area:

The macro scale (1:50,000) landslide susceptibility map (LSM) is a useful geo-information tools that can be adopted for perspective Land use planning and zoning regulations. It is presented with susceptibility classes in bright and discerning colors (like red for 'High'; green for 'Moderate' and yellow for 'Low' susceptibility) with all major roads, important locations, and major civil infrastructures along with plotting of all the observed historical landslide locations (Fig 6).

In toposheet 53E/01 high susceptible slopes are along Hurla valley, Lag valley and near Parashar Lake and in toposheet 53E/02 around Larji, Thalot, Hanogi, Pandoh area along NH-21. Besides, some sporadic patches a prominent concentration of high class is scattered over areas of 53E/01 & 53E/2

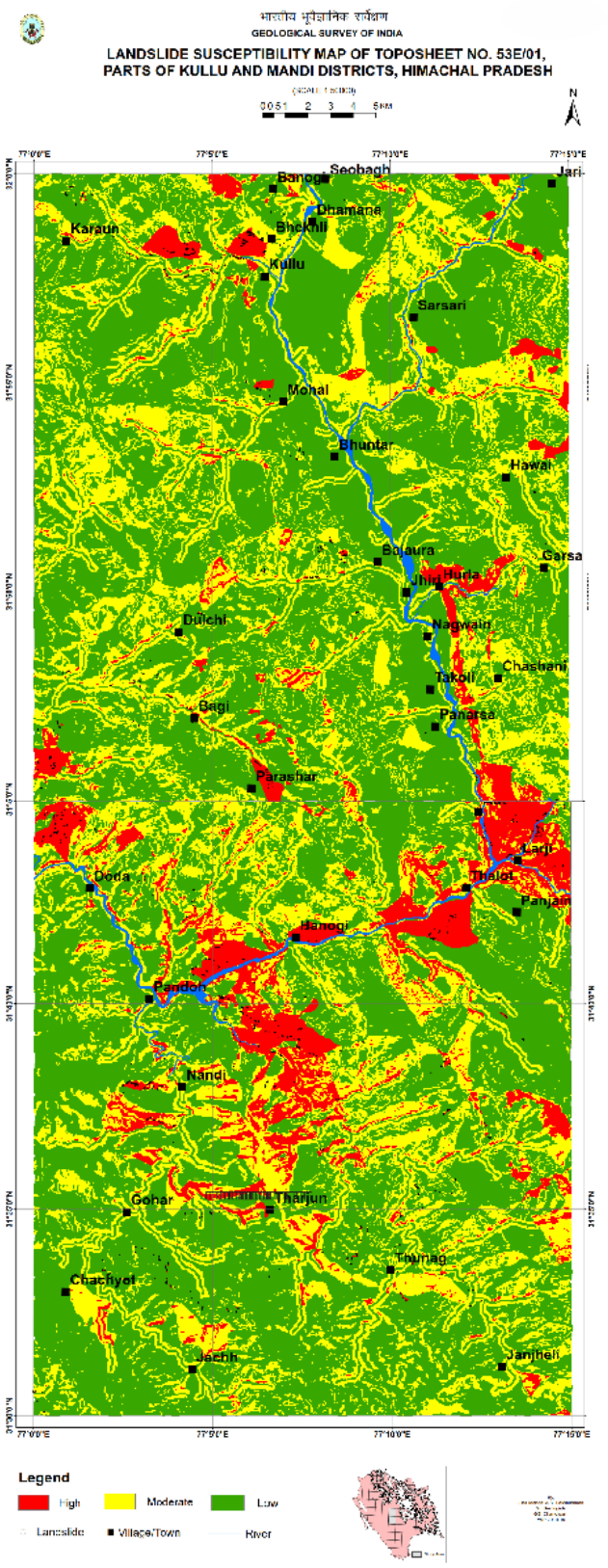

Figure 6 Susceptibility map of T.S. 53E/1 & 2, parts of Kullu and Mandi, H.P

4.4.1 Major zones and vulnerability associated with them:

Based on the susceptibility map, an attempt was made to better understand the vulnerability associated with the areas under high susceptibility zones by delineating the area sector (Valley) wise.

Sector 1
Sarwari Khad (Lag Valley) – North-north western part of toposheet 53E/1:

Sarwari Khad is one of significant tributary of Beas River in the study area that flows SSE and eastward initially and confluences with Beas at Kullu township. The valley exhibits important villages like Bhutti, Shalang, Dubkan, Tandari, Gadiyara, Khalar, Bastori etc. Geologically the initially reaches of the valley are formed by streaky banded gnessis, kyanite bearing schist and quartzites of Vaikirta and Manjir formations . The inference from LULC map reveals that the valley is been predominately occupied by agricultural land. Very interesting thing that can be observed was that high susceptible zones demarcated by red colour, which matches with the Geomorphology factor that smacks these spot by denudational hill slopes. The field observations indicate with the addition of widening up of state highway road there by the slopes equilibrium has been disturbed which adds more weightage to this particular geofactor class.

Moderate susceptible zone covers about 30% (656 km^2) of study area. The moderate class occurs along the periphery surrounding the high susceptible slopes.

Sector 2
Hurla Nala (Garsa valley) – Located on the south-east mid lower portion of TS 53E/1:

Hurla Nala is a very prominent tributary of river Beas. Hurla nala flows E-W within Garsa valley and confluence with Beas few metres upstream of Nagwain. Geologicaly the area constitutes Grey dolomites, purple green limestones, white quartzites, shale and phyllite of Aut and Hurla formations. Geomorphologically, the valley appears to have strong structural control. The presence of resistance rock types results as steep rocky slopes, High to moderately dissected hill slopes which make the slope potentially vulnerable for rock slides. The slopes are covered with debris and slope water materials. The area is been categorized under moderate to high susceptible in the susceptibility map. The presence of highly jointed quartzite-phyllites within moderate to steep slopes and escarpments supplements the slopes to form stable and unstable wedges along with planar face on the day lighting slopes (Fig 7). In addition road cuts poor support walls and mining activity aggravates the susceptibility rating to moderate to high.

Figure 7 Plane failure (rock cum debri) slide along Hurla Valley

Sector 3
Larji to Pandoh. Beas River valley. Northern part of TS 53E/2:

Larji to Pandoh stretch is steep narrow gorge is the evidence of strong structural control of the area. Beas River flows ENE to WSW (Fig 5.7). The zone is composed of pebbly slate, gritty quartzite phyllite of Manjir Formation, Carbonaceous slate, phyllite and subordinate limestone of Katarigali Formation, and Quartzite, phyllite, slate, schist, thin bands of gneiss of Vaikrita Formation. The differential lithologic composition and differential competency of the material along with the presence of a major synform trending NNW-SSE with highly jointed rock mass made this zone to high vulnerable zone or landslides. The incidence of recent Dwada rockslide also falls within this stretch (Fig 4.12). The slates near Hanogi mata temple are dislodged with open joints appear to be stacked over one other. This zone is high susceptible zone and good magnitudes of earthquake tremor / heavy rainfall are sufficient to trigger landslides along this zone.

Figure 4.12 Alternate layers phyllitic slate, quartzite biotite schist with (3+1) major joint sets with downstream dipping foliation.

Sector 4
Bagi-Parashar:

The area surrounding Parashar lake remain under snow cover during winter. The rock type is Phyllitic chloritic schist with ~ 2-5 m thick insitu clay rich soil. There are also presences of four small lakes observed around the area. During rainy season material charged with water exceeds infiltration capacity over flow and results ditches, puddles. (Fig. 4.13) The slide recorded along Bajaura and Parashar road, where debris slides reported triggered by cloud burst resulting in breach of a bridge along with 300m stretch of road and settlements along with loss of life in 2014. The 5-7 m thick moraine deposits of glacio-fluvial origin was the source of the slide identified u/s near Parashar Lake at El ±2785m above msl. The Google image also indicated series of detachment blocks of soil leading to slide due to steep gradient towards the downhill slope/stream. Creep action was also observed.

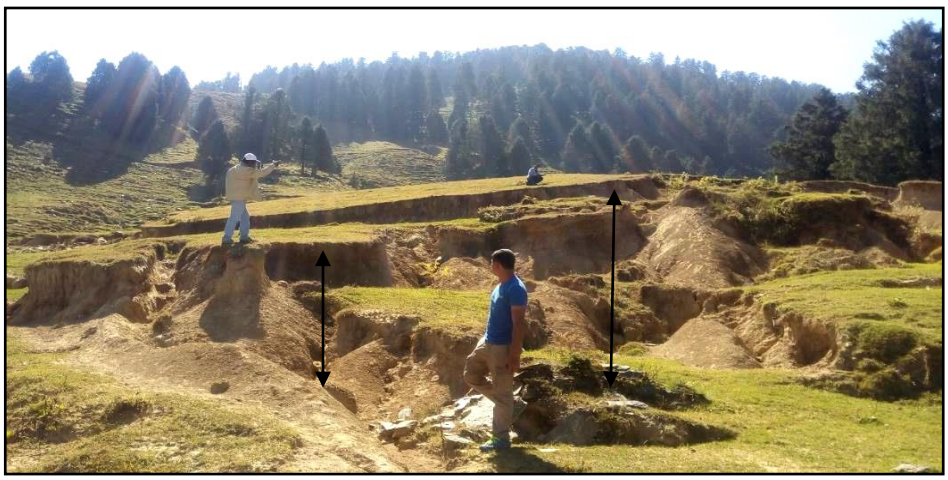

Figure 4.13 Thick in-situ clay rich soil of 2-5 m with tension cracks near Parashar Lake

5. Conclusions:

The susceptibility model is used to delineate the spatial distribution of potential landslide areas with varying degree of proneness to sliding, based on certain assumptions. It is based on the principle of "Present is the key to the past" i.e. the landslides will occur in future under the same conditions and triggering factors that produced them in past. It is expected that the existing geo-environmental conditions may change as per change in Land use pattern, hydrological conditions due to human action. Conditions may also change when the source of a landslide is exhausted or the morphology of the slope is changed and becomes stable. However, it is to be mentioned that to some extent the assumption holds true but preparatory factors (e.g., slope, aspect, curvature, geomorphology and drainage) are not expected to change significantly in coming few decades. All the geofactor maps like geomorphology, SFM and LULC prepared using remote sensing data were also subjected to detailed field observations and validations at accessible locations. The analyses revealed the geofactors in their decreasing order their Predictor Rating (PR) i.e. with respect to landslide favorability as LULC (PR-9), Geomorphology (PR-7), SFM (PR-7), Thickness (PR-5), Drainage (PR-3), Slope (PR-2)

and Curvature and Fault/Fracture (PR-1), which were together processed in ILWIS to obtain a Success Rate Curve to derive the final Landslide Susceptibility Map dividing the study area in to 'High', 'Moderate' and 'Low' susceptibility zones. In study area, about 85% cumulative distribution of all landslide source areas is contained within 20% of the study area having higher susceptibility scores. The next 90% of cumulative landslides are contained within 30% of the study area. The derived susceptibility map is an estimate of an area indicating relative proneness to landslide. The predictions of time and magnitude of event, hazard and risk aspects of landslides / zones is beyond the scope of the present study. The present study has been taken up after increasing recognition of socio-economic impacts of landslide, and is a prerequisite to evaluation of hazard and effective mitigation for long sustainable development of the area.

References:

1. Aleotti, P. and Chowdhury, R. (1999), "Landslide Hazard Assessment: Summary Review and New Perspectives", Bulletins of Engineering Geology and the Environment, 58(1), pp 21-44.
2. Anabalagan, R., (1992): Landslide hazard evaluation and zonation mapping in mountainous terrain, *Engineering Geology*, 32:269–277.
3. Baeza, C. and Corominas, J. (2001): Assessment of shallow landslide susceptibility by means of multivariate statistical techniques. Earth surface processes and landforms, 26: 1251- 1263.
4. Bonham-Carter, G.F. (1994): Geographic Information Systems for Geoscientists: Modeling with GIS. Pergamon, Elsevier Science Ltd., 398 pp.
5. Burrard, S.G. and Hayden, H.H. (1933), "A Sketch of Geography and Geology of the Himalaya Mountains and Tibet-Part II". Delhi.
6. Carrara A., Cardinali M., Guzzetti F., 1992. Uncertainty in assessing landslide hazard and risk. ITC Journal 2, 172-183.
7. Chandel, V. B. S., Brar, K. K. and Chauhan, Y. (2011): RS & GIS Based Landslide Hazard Zonation of Mountainous Terrains A Study from Middle Himalayan Kulu District, Himachal Pradesh, India. International Journal of Geomatics and Geosciences Volume 2, No 1, 2011, pp 121-132.
8. Chung, C.-J.F., Fabbri, A.G. and van Westen, C.J. (1995): Multivariate regression analysis for landslide hazard zonation. Kluwer Academic Publishers, Netherlands, pp. 107-133.
9. Chung C.J., Fabbri A.G. (1999): Probabilistic prediction models for landslide hazard mapping. Photogrammetric Engineering and Remote Sensing 65 (12), 1389–1399.
10. Chung C.J., Fabbri A.G., 2003. Validation of spatial prediction models for landslide hazard mapping. Natural Hazards 30, 451-472.
11. Crozier, M.J., (1986): *Landslides: Causes, Consequences and Environment*, Croom Helm Australia Pty. Ltd., London, United Kingdom, 252 p.
12. DeRose R.C., Trustrum N.A. and Blaschke P.M. (1991): Geomorphic change implied by regolith - Slope relationships on steep land hill slopes, Taranaki, New Zealand. Catena, 18 (5): 489-514.

13. Deshpande P. K., Patil, J. R., Nainwal, D. C. and Kulkarni, M. B. (2009): Landslide hazard zonation mapping in Gopeshwar, Pipalkoti and Nandprayag areas of Uttarakhand. IGC 2009, Guntur, India, pp. 808-812.
14. Dietrich W.E., Wilson C.J. and Reneau S.L., Hollows, (1986): Colluvium and landslides in soil- mantled landscapes. In: A.D. Abrahams (Editor), Hill slope Processes. Allen and Unwin, Boston, pp. 361-386.
15. Gajbhiye P. K. and Rajkumar, M. (2015): A report on macro-scale (1:50,000) Landslide Susceptibility Mapping in parts of toposheets no. 53J/6, 53J/9, 53I/12 and 53I/16, Tehri Garhwal and Uttarkashi districts, Uttarakhand. (Unpublished GSI report, FS 2014-15)
16. Gemitzi, A., Falalakis, G., Eskioglou, P. and Petalas, C. (2011): Evaluating landslide susceptibility using environmental factors, fuzzy membership functions and GIS. Global Nest Journal, Vol 13, No 1, pp 28-40, 2011.
17. Ghosh, S., Carranza, E.J.M., van Westen, C.J., Jetten, V.G. and Bhattacharya, D.N., 2011. Selecting and weighting spatial predictors for empirical modeling of landslide susceptibility in the Darjeeling Himalayas (India). Geomorphology, 131 (1–2): 35-56.
18. Ghosh, S., Westen, C.J., Carranza, E.J.M., Jetten, V.G., Cardinali, M., Rossi, M. and Guzzeti, F. (2012): Generating event-based landslide maps in a data-scarce Himalayan environment for estimating temporal and magnitude probabilities. ELSEVIER Engineering Geology 128 (2012) pp. 49-62.
19. Ghosh, S., Kumar, A. and Bora, A. (2014): Analyzing the stability of a failing rock lope for suggestingsuitable mitigation measure: a case study from the Theng rockslide, Sikkim Himalayas, India. Bulletin of Engineering Geology and the Environment. Springer.
20. Guzzetti F., Carrara A., Cardinali M., Reichenbach P., 1999. Landslide hazard evaluation: a review of current techniques and their application in a multi-scale study, Central Italy. Geomorphology 31, 181–216.
21. Guzzetti F., Reichenbach P., Cardinali M., Galli M., Ardizzonem F., 2005. Probabilistic landslide hazard assessment at the basin scale. Geomorphology 72, 272– 299.
22. Hanley, J.A. and McNeil, B.J., (1982): The meaning and use of the area under a receiver operating characteristic (ROC) curve. Radiology, 143 (1): 29-36.
23. Krishnan M.S. (1982). *Geology of India and Burma*, CBS Publishers, Delhi.
24. Kumar, P. (2012): Post disaster studies of landslide occurrences on 26th february 2011 and 4th - 5th March 2011 at different places along NH-21 in Himachal Pradesh. (Unpublished GSI report, FS 2010-12)
25. Sah, M.P. & R.K. Mazari. (2007), "An Overview of the Geoenvironmental Status of the Kulu Valley, Himachal Pradesh, India". Journal of Mountain Science, 4(1), pp 3- 23.
26. Sarkar, S. and Kanungo, D.P. (2004): An integrated approach for Landslide Susceptibility Mapping using remote sensing and GIS. Photogrammetric Engineering & Remote Sensing Vol. 70, No. 5, May 2004, pp. 617–625.
27. Sarkar, S, Kanungo, D.P., Patra, A.K. and Kumar, P. (2006): GIS based Landslide Susceptibility Mapping — a case study in Indian Himalaya.

Bibliography:

1. Gupta SK, 1981-82,"Progress report No.1 On Landslide Zonation in Mountainous region of Himachal Pradesh" GSI Unpublished report.
2. Gupta SK, 1981-82,"Progress report No.2 On Landslide Zonation in Mountainous region of Himachal Pradesh" GSI Unpublished report.
3. Chengal Raju KC, 1959 -60, "Geological report on the investigation of the slip and subsidence in Shimla."
4. Sirvastava J.P, 1957-58" Report on the investigation of foundation condition of stability of hill slide on the Snowdon hospital of Himachal Pradesh, Simla."
5. Srivatava K.N and Tikku A.K, 1965-66" Geological report on the investiongation of reported subsidence in Simla area."
6. Prasad V, 1962-63 "A Geological Note on the reconnaissance of the landslide along the Kirathpur –Bilaspur road, Himachal Pradesh and its relation to Bhakar reservoir."
7. Auden J.B, 1951 "Geological note on Slips and Subsidence in Simla"
8. Srivatava K.N, 1967-68 "A note on the examination of the reported subsidence of a portion of the Solan – Menus road in Solan town"
9. Sharma VK, 2005-06 "Landslide macro zonation of Shimal area with special reference to slope stability."
10. Singh G, 1981-81 "Progress report No.4 On the Geotechincal mapping of Shimal area H.P"
11. Mehta JS and Kumar Pankaj, 2004-06 "Landslide Hazard zonation mapping in Ravi basin, Chamba district, Himachal Pradesh"